Influence of order in stepwise electroless deposition on anode properties of thick-film electrodes consisting of Si particles coated with Ni and Cu

*Hiroyuki Usui, Naoki Uchida, and Hiroki Sakaguchi**

Department of Chemistry and Biotechnology, Graduate School of Engineering, Tottori University

4-101 Minami, Koyama-cho, Tottori 680-8552, Japan

*Corresponding author. Tel./Fax: +81-857-31-5265; e-mail: sakaguch@chem.tottori-u.ac.jp

Keywords: Si anode, Thick-film electrode, Electroless deposition, Gas deposition, Li-ion battery

Abstract

Nickel and copper were coated on Si particles by a stepwise electroless deposition technique in which the coating orders of the metals were exchanged. Thick-film electrodes for Li-ion batteries were prepared by a gas-deposition method using the coated Si particles, and the anode performance of these electrodes was investigated. For (Cu, Ni)-coated Si particles obtained by primary Cu deposition and successive Ni deposition, Cu and Ni metal layers were individually deposited on the Si particles. In contrast, in case of (Ni, Cu)-coated Si particles prepared by primary Ni deposition, Cu layer stacked on Ni layer owing to a high catalytic activity of Ni, forming a thicker coated layer. The latter electrode exhibited notably improved performance with the discharge capacities over 1000 mA h g^{-1} maintained until 400th cycle. The layer stack of Cu on Ni is probably effective for a release of a stress from the Si particles during charge–discharge reactions.

1. Introduction

For the popularization of developing electric vehicles, next-generation Li-ion batteries with a high-energy density over 500 Wh kg^{-1} are urgently aspired. A large specific capacity exceeding 1600 mA h g^{-1} is required for next-generation anode materials on the assumption of 300 mA h g^{-1} for a cathode specific capacity and 3.7 V for an electromotive force. However, it is very difficult to apply practically-used anodes of graphite-based materials to the electric vehicles because the theoretical capacity of graphite is only 372 mA h g^{-1}. Silicon is one of the most attractive materials for the anode of next-generation Li-ion batteries because the theoretical capacity of Si (~4200 mA h g^{-1}) is much larger than that of graphite. The remarkably large capacity is originated from an alloying reaction of Li–Si in the composition range from Si to $Li_{4.4}Si$ [1-3]. On the other hand, Si has some critical disadvantages as anode material, a high electrical resistivity, a low diffusion coefficient of Li ion in Si, and a drastic change of specific volume during the alloying/dealloying reactions. The volumetric change ratio per Si atom corresponds to be 410% [4], which causes a breakup of the electrode and an electrical isolation of the active material of Si. Consequently, the electrode performance of Si anode rapidly fades away by repeating Li-insertion and Li-extraction. When a silicide instead of elemental Si is utilized as the active material of anode, the capacity is drastically lost owing to smaller storage amount of Li ions in the silicide. Therefore, we believe that anodes for the next-generation Li-ion battery should mainly consist of elemental Si to derive an advantage of its larger theoretical capacity.

To overcome the disadvantages of Si anodes, some researchers have proposed composite anodes using elemental Si. Ishikawa *et al.* have investigated Si–Ni–C composites synthesized by a two-step mechanical milling process [5]. Chen *et al.* have obtained a good performance for an anode of Cu foam-supported Si film formed by a radio-frequency magnetron sputtering [6]. Cuevas *et al.* have proposed nanostructured Si/Sn–Ni/C composites prepared by a mechanical milling process [7]. Takeda *et al.* have reported that Si–C composite anodes prepared by thermal decomposition of polyvinylchloride exhibited an improved electrode performance [8]. On the other hand, the authors

have synthesized composite active materials consisting of elemental Si and metals/alloys, and have investigated anode properties of thick-film electrodes obtained by a gas-deposition (GD) method using the composite active materials. It has been discovered that the electrode performance is significantly improved by the synergetic effects of the properties of elemental Si and combined metals/alloys [9-14]. In particular, we have found excellent cycling performance for a thick-film electrode consisting of Ru-coated Si particles prepared by electroless deposition (ELD) [12]. Elemental Ru is, however, not suitable for practical use owing to its rarity and expensiveness. Thus, we have prepared thick-film electrodes of the coated Si particles in which Ru was replaced with more inexpensive metals of Cu or Ni, and have confirmed that the electrode of Cu-coated Si [13] and Ni-coated Si [14] also exhibited noteworthy electrode performance. The results suggest that these coated metal layers on the Si particles can play important roles in increasing the electrical conductivity of the active material [13] and in releasing a stress induced by the volumetric changes of Si [14].

The cycling performance of the two electrodes using Cu-coated Si and Ni-coated Si was comparable. It is well known that standard electrode potential of –0.25 V vs. SHE (standard hydrogen electrode) for Ni/Ni^{2+} is much higher than that of +0.34 V vs. SHE for Cu/Cu^{2+} at room temperature. This means that Ni^{2+} ions are electrochemically more active in comparison with Cu^{2+} ions. In addition, an ELD of Ni is autocatalytic reaction with a high reactivity [15]. Thus, we expect that a reducing agent of ELD is actively oxidized on Ni layer deposited onto Si particles, and that metal ions are easily reduced on the Ni layer to form a thicker layer of coated metals. We are herewith suggesting a stepwise ELD technique of Ni and Cu on Si particles for preparation of the thick-film anodes. In this study, we carried out the stepwise ELD of Ni and Cu on Si particles exchanging the ELD order, and investigated the anode properties for the thick-film electrodes obtained by the GD method using the Si particles coated by stepwise ELD.

2. Experimental

A stepwise electroless deposition was carried out at room temperature to individually coat Ni and Cu layers on Si particles in this study. Firstly, $NiSO_4 \cdot 5H_2O$ of 0.0425 g and commercial Si particles (Wako Pure Chemical Industries, Ltd., 99.9%) were added in 0.1 mol/L (M) H_2SO_4 aqueous solution under a vigorous stirring of 500 rpm. The pH value of the solution was approximately 1.5. As a reducing agent, 1.3 mM $NaBH_4$ aqueous solution of 50 ml was added to the solution to reduce Ni^{2+} ions. The obtained Ni-coated Si particles were washed with distilled water and were dried in air for 12 hours. Next, the Ni-coated Si particles and $CuSO_4 \cdot 5H_2O$ of 0.036 g were added in 0.1 M H_2SO_4 aqueous solution under the stirring. And then, the $NaBH_4$ solution of 50 ml was added in the solution to reduce Cu^{2+} ions. After the drying process, we obtained Si particles coated with Ni and Cu. Hereafter, we will call the particles (Ni, Cu)-coated Si particles in the sense that Ni was firstly coated on the Si particles and Cu was secondarily deposited on the Ni-coated Si particles. The elemental analysis of the coated particles was carried out by inductively coupled plasma atomic emission spectroscopy (ICP-AES, Spectro Ciros CCD, Rigaku Ltd.). We detected 95.0 wt.% Si, 2.2 wt.% Ni, and 2.8 wt.% Cu, and thus the total coated amount was approximately 6.0 wt.%. On the other hand, (Cu, Ni)-coated Si particles were also prepared by exchanging the order of ELD for Ni and Cu. The elemental analysis revealed that the particles contain 94.2 wt.% Si, 2.8 wt.% Ni, and 3.0.wt % Cu. The total coated amount of 5.8 wt.% in the (Cu, Ni)-coated Si particles is nearly identical to that of 6.0 wt.% in the (Ni, Cu)-coated Si particles. The elemental distribution and nanostructure of the coated Si particles were observed by a scanning electron microscope (SEM, JSM-5200, JEOL Ltd.) equipped with an energy dispersive X-ray spectroscope (EDS, EDS-54033MCK, JEOL Ltd.) and a transmission electron microscope (TEM, JEOL-2010, JEOL Ltd.).

For gas-deposition, Cu foil substrates with 20 μm in thickness were set up in a guide tube with a nozzle of 0.8 mm diameter in a vacuum chamber [9-14,16]. The distance from the nozzle to the substrate was set to be 10 mm. An aerosol consisting of Ar gas (differential pressure: 7×10^5 Pa) and

active material powders of the coated Si was generated in the guide tube, and instantly gushed from the nozzle onto the Cu substrate in the chamber with a base pressure of 8 Pa. The weight of the deposited active materials on the substrate was 0.028–0.039 mg. The film thickness of the deposited active materials was not uniform but was 1–4 μm.

Electrochemical measurements were carried out with a beaker-type three-electrode cell. The working electrodes were the obtained thick-film electrodes. Both counter and reference electrodes were 1-mm-thick Li metal sheets (Rare Metallic, 99.90%). We used $LiClO_4$-dissolved in propylene carbonate (PC; $C_4H_6O_3$, Kishida Chemical Co., Ltd.) at concentration of 1.0 M as the electrolyte. Constant current charge–discharge tests were performed using an electrochemical measurement system (HZ-3000 Hokuto Denko Co., Ltd.) under a constant current of 0.05 mA (current density: 1.66–1.78 A g^{-1}, C rate: 0.40–0.42 *C*) at 303 K with the cutoff potentials set as 0.005 V vs. Li/Li^+ for charge and 3.400 V vs. Li/Li^+ for discharge.

3. Results and Discussion

Figure 1 gives charge-discharge curves at the first cycles for thick-film electrodes consisting of (Cu, Ni)-coated and (Ni, Cu)-coated Si particles. For comparison, the curve was also drawn for the electrode consisting of *pristine* Si particles without ELD coating. In the Li–Si alloy system, four equilibrium charge-discharge potentials have been reported for four kinds of binary alloy phases, $Li_{12}Si_7$ ($Li_{1.71}Si$), Li_7Si_3 ($Li_{2.33}Si$), $Li_{13}Si_4$ ($Li_{3.25}Si$), and $Li_{22}Si_5$ ($Li_{4.4}Si$) [17,18]. In this study, only one plateau appeared at the potentials of about 0.1 and 0.4 V vs. Li/Li^+ during the charge and discharge reactions in every case, which is presumably due to the low diffusion coefficient of Li ions in Si and the kinetic effect of the measurement [19]. Thus, we confirmed alloying/dealloying reactions of Li–Si in the electrodes of (Cu, Ni)-coated Si and (Ni, Cu)-coated Si. The potential difference between the plateaus was approximately 0.3 V, which corresponds to the difference of

0.23–0.27 V between the equilibrium charge and discharge potentials in $Li_{12}Si_7$, Li_7Si_3, and $Li_{13}Si_4$ phases [20]. These potential differences are attributed to a polarization of the cell [19].

Large initial irreversible capacities were observed. For instance, the pristine Si electrode showed approximately 3000 and 2000 mA h g^{-1} of the charge and discharge capacities at the first cycle. The large capacity loss is mainly attributed to the pulverization of Si induced by its volumetric change during the charge-discharge. Even in the first charge process, the drastic volume expansion leads to the pulverization and the electrical isolation of Si, which decreases a portion of the active material contributing to Li-storage. Similarly in the first discharge process, the volumetric shrinkage brings on the pulverization and the electrical isolation. Therefore, the charge and discharge capacities at the first cycle become much lower than silicon's theoretical capacity of 4200 mA h g^{-1}.

Figure 2 shows dependence of the discharge (Li-extraction) capacity on charge-discharge cycling number for each thick-film electrode mentioned in Fig.1. For comparison, the figure shows the capacity variation of Cu-coated Si [13] and Ni-coated Si electrodes with the same deposition amount of 6 wt %. The electrode of pristine Si showed the initial capacity of 2000 mA h g^{-1} and a rapid capacity decay until the 100th cycle, resulting in poor electrode performance. The pristine Si electrode has a low elastic modulus [14], and cannot easily release the stress induced by the volumetric changes in Si during alloying and dealloying of Li–Si, and thus the electrode shows a drastic pulverization and an electrical isolation of the active material film in an earlier stage of charge–discharge cycles. On the other hand, the Cu-coated Si and Ni-coated Si electrodes exhibited smaller initial capacities of 870 [13] and 1130 mA h g^{-1} [14], respectively. The two electrodes, however, showed very stable capacity retention after 100th cycle. For the reason of the stable cycling performance, we have reported that the coated metal layers on the Si can play important roles in increasing the electrical conductivity of the active material [13] and in releasing the stress induced by the volumetric changes of Si [14]. The two electrodes of (Cu, Ni)-coated Si and (Ni, Cu)-coated Si, obtained by the stepwise ELD in this study, demonstrated larger initial capacities of 1740 and 1380

mA h g^{-1} in comparison with the Cu-coated Si and Ni-coated Si electrodes. It should be noted that Ni and Cu are inactive metals for Li, and that the Cu and Ni layers prevent Li ions from inserting and extracting in/from Si particles if the particle surface was completely covered with the layers. The stepwise ELD is expected to enable Cu and Ni layers to laminate because the metal ions were reduced in twice by the reducing agents. The Si particles of these electrodes would have a larger uncoated surface because Cu and Ni formed the stacked layers partially or completely. Thus, the larger uncoated surface area of the (Cu, Ni)-coated Si and (Ni, Cu)-coated Si leads to efficient Li-insertion and Li-extraction, thereby increasing these initial discharge capacities. The capacity of (Cu, Ni)-coated Si electrode, however, steeply dropped during the initial 100 cycles, and the cycling performance after 400th cycle is comparable to that of the Cu-coated Si and Ni-coated Si electrodes. By contrast, it is noteworthy that the (Ni, Cu)-coated Si electrode maintained very large capacities over 1000 mA h g^{-1} until the 400th cycle though the capacity decay could not be avoided in the initial 50 cycles and after 400th cycle. There is no difference in the total coated amounts between (Cu, Ni)-coated Si and (Ni, Cu)-coated Si electrodes. Nevertheless, a markedly different performance was obtained only by exchanging the coating order of Ni and Cu in the stepwise ELD, which is a very notable result. We infer that the electrode performance was different because the coating order affects the morphology of coated layer on the Si particles.

Figures 3(a) and 3(b_1) display TEM images of the (Cu, Ni)-coated Si particle prepared by the stepwise ELD. An angular particle with size of several hundred nanometers was confirmed to be crystalline Si by the analysis using selected area electron diffraction (SAED). As shown in Fig. 3(a), we can see that many smaller particles with size ranging from 50 to 200 nm were attached on the Si particle. The surface of the Si particles was partially exposed. The exposed Si surface is essentially important for use as an anode active material because the alloying/dealloying reactions of Li–Si do not efficiently occur if the Si surface is completely covered with inactive metals such as Cu and Ni. Figure 3(b_2) represents a SAED pattern obtained for a region shown in Fig. 3(b_1). Diffraction spots

assigned as Si (JCPDS No. 27-1402) and Cu (JCPDS No. 04-0836) appeared. This result obviously demonstrated that elemental Cu particles were individually deposited on the Si surface. On the other hand, the diffraction spots of Ni (JCPDS No. 87-0712) were also confirmed in addition to those of Si and Cu (Fig. 3(c)) when the SAED analysis was performed for a broader region of the particle shown in Fig. 3(a). Therefore, in a submicron scale, it is suggested that elemental Cu and Ni were separately deposited on the Si surface.

To elucidate a more macroscopic morphology of the coated layer, we discuss results of SEM-EDS analysis. Figure 4(a_1) shows a SEM image of the (Cu, Ni)-coated Si particles. We observed aggregated large particles. Figures 4(a_2) and 4(a_3) display corresponding element mapping for CuKα and NiKα, respectively. Both elemental Cu and Ni were uniformly detected on overall region of the Si particle. Figures 4(b_1), 4(b_2), and 4(b_3) depict a SEM image and corresponding element mapping for CuKα and NiKα of the (Ni, Cu)-coated Si electrode which has exhibited an excellent cycling performance until 400th cycle in Fig. 2. The SEM-EDS mapping clearly revealed that Cu was locally deposited on the Si particles. In contrast, NiKα could not be observed though the existence of 2.8 wt. % Ni was confirmed for the particles by the ICP analysis, indicating that Cu layer of several hundred nanometers in thickness was stacked on Ni layer. We expect that the Ni thickness is also several hundred nanometers because the deposited amount of Cu is comparable to that of Ni. It is considered that metallic Cu is preferentially deposited not on Si surface but on Ni layer in the secondary ELD process. The phenomenon is related to catalytic activities of metals for the oxidation of the reducing agent, $NaBH_4$. The catalytic activity of Ni for $NaBH_4$ is much higher than that of Cu [15, 21]. We consider a following process for the (Ni, Cu)-coated Si. Once Ni deposits on any active sites of Si surface at the beginning of the first ELD, the reducing agent of $NaBH_4$ is preferentially oxidized on the surface of Ni owing to its high autocatalytic effect, resulting in a successive deposition of Ni on the Ni layer. In the secondary ELD, Cu is preferentially deposited on the Ni layer because $NaBH_4$ is oxidized on the Ni layer surface. Once deposited, Cu^{2+} ions are

reduced on the Cu layer due to an autocatalytic effect of Cu. Consequently, in case of the stepwise ELD for the (Ni, Cu)-coated Si, Ni is locally deposited on the Si surface, and Cu is selectively deposited on the Ni layer. In contrast, another deposition process is suggested for the (Cu, Ni)-coated Si. Cu exhibits the autocatalytic effect, but the activity is lower than that of Ni [21]. After Cu deposited once at the beginning of the first ELD, successive Cu deposition occurs on the nucleated Cu layer and on Si surface because the oxidation reaction of $NaBH_4$ takes place not only on the Cu layer but also on Si surface owing to the lower autocatalytic effect. This is a reason why Cu element was more uniformly detected on the Si surface in the Fig. 4(a_2). In the secondary ELD, $NaBH_4$ is oxidized on the Cu layer surface and on an uncoated Si surface. In consequence, Ni and Cu were separately deposited though Ni layer occasionally deposited on the Cu layer.

The coated layer of the (Ni, Cu)-coated Si particles is possibly thicker due to stacking of Cu layer on Ni layer in comparison with the other electrodes, Cu-coated Si, Ni-coated Si, and (Cu, Ni)-coated Si electrodes. Thus, it is suggested that the stacked (Ni, Cu) layers on the Si particles are effective for the release of the stress from Si particles, and that the stacked layers showed superb mechanical durability for a long time up to 400th cycle. We can easily expect that the surface of Si particles is not perfectly covered because metallic Cu is preferentially deposited on Ni layer, which leads to efficient alloying/dealloying reactions of Li–Si. The selectivity of deposition sites for coated metals in the ELD process is critically important to control deposition area and deposition thickness.

Figure 5 shows coulombic efficiencies of the thick-film electrodes consisting of (Cu, Ni)-coated Si, (Ni, Cu)-coated Si, and pristine Si particles in the initial 200 cycles. The first coulombic efficiencies for the three electrodes were 58%, 55%, and 65%, respectively. On the other hand, the first efficiencies of 66% and 46% have been observed for the Cu-coated Si and Ni-coated Si electrodes (not shown in the figure). It is considered that there is no significant difference in the first efficiencies. However, from the 10th cycle to 40th cycle, a significant dropping of the efficiency was observed for the pristine Si electrode. The lowered efficiency indicates a larger irreversible capacity

originated in the physical detachment and the electrical isolation of the active material from the substrate of the current collector. We can clearly recognize that the efficiency dropping was substantially suppressed for two kinds of the coated Si electrodes by the stepwise ELD in this study. The reason is that irreversible capacities were reduced because of the improved electrical conductivity [13] and the enhanced mechanical durability [14] by the coated metal layers on Si. Among the two electrodes, the (Ni, Cu)-coated Si electrode maintained higher efficiencies in comparison with the other electrode after the 10th cycle. This implies that the stacked (Ni, Cu) layers on the Si particles are more effective for enhancing the mechanical durability. Consequently, the stepwise ELD technique seems to be a very interesting approach to prepare a source active material of coated Si particles for GD thick-film electrodes which have both large capacity and excellent cycling performance.

4. Conclusion

In this study, we coated Si particles with Ni and Cu by the stepwise ELD technique in which the coating orders of Ni and Cu were exchanged, and prepared the thick-film electrodes by the GD method using the coated-Si particles. The nanostructure and elemental distribution of the coated particles were observed by the TEM and the EDS mapping analysis. The TEM observations revealed that metallic Cu and Ni were individually deposited on the surface of Si particles for the (Cu, Ni)-coated Si particles which were obtained by primary ELD of Cu and successive ELD of Ni. In contrast, the EDS mapping result suggested that Cu layer stacked on Ni layer to form a thicker coated layer in case of the (Ni, Cu)-coated Si particles prepared by primary ELD of Ni. Because of the stacked layer, the thick-film electrode of (Ni, Cu)-coated Si particles exhibited notably improved performance with the discharge capacities over 1000 mA h g^{-1} until 400th cycle. It is thus suggested that the stacked layer of (Ni, Cu) on the Si particles is effective for the release of the stress from Si particles induced by the volumetric change of Si during charge-discharge reactions.

Acknowledgments

This work was supported in part by the Li-EAD program of the New Energy and Industrial Technology Development Organization (NEDO) of Japan. This work has been partially supported by a Grant-in-Aid for Scientific Research from the Ministry of Education, Culture, Sports, Science and Technology (MEXT) of Japan. The authors also gratefully acknowledge Prof. K. Ichino for his kind assistance with TEM observations. The authors thank Dr. T. Iida and Mr. M. Shibata for their patient assistance with electroless deposition. The authors would like to thank the reviewer for his/her appropriate suggestions and helpful comments.

References

[1] J. O. Besenhard. J. Yang, M. Winter, *J. Power Sources*, 68 (1997) 87.

[2] U. Kasavajjula, C. S. Wang, A. J. Appleby, *J. Power Sources*, 163 (2007) 1003.

[3] N. Ding, J. Xu, Y. Yao, G. Wegner, I. Lieberwirth, C. Chena, *J. Power Source*s, 192 (2009) 644.

[4] C. J. Wen, R. A. Huggins, *J. Solid State Chem.*, 37 (1981) 271.

[5] T. Sugimoto, Y. Atsumi, M. Kono, M. Kikuta, E. Ishiko, M. Yamagata, M. Ishikawa, *J. Power Source*s, 195 (2010) 6153.

[6] H. Li, F. Cheng, Z. Zhu, H. Bai, Z. Tao, J. Chen, *J. Alloys Compd.*, 509 (2011) 2919.

[7] Z. Edfouf, F. Cuevas, M. Latroche, C. Georges, C. Jordy, T. Hézèque, G. Caillon, J. C. Jumas, M. T. Sougrati, *J. Power Source*s, 196 (2011) 4762.

[8] Q. Si, K. Hanai, N. Imanishi, M. Kubo, A. Hirano, Y. Takeda, O. Yamamoto, *J. Power Source*s, 189 (2009) 761.

[9] H. Sakaguchi, T. Toda, Y. Nagao, T. Esaka, *Electrochem. Solid-State Lett*., 10 (2007) J146.

[10] T. Iida, T. Hirono, N. Shibamura, H. Sakaguchi, *Electrochemistry*, 76 (2008) 644.

[11] H. Sakaguchi, T. Iida, M. Itoh, N. Shibamura, T. Hirono, *IOP Conf. Series: Mater. Sci. Eng*., 1 (2009) 012030.

[12] H. Usui, Y. Kashiwa, T. Iida, H. Sakaguchi, *J. Power Sources*, 195 (2010) 3649.

[13] H. Usui, H. Nishinami, T. Iida, H. Sakaguchi, *Electrochemistry*, 78 (2010) 329.

[14] H. Usui, M. Shibata, K. Nakai, H. Sakaguchi, *J. Power Sources*, 196 (2011) 2143.

[15] Y. Yamauchi, T. Momma, T. Yokoshima, K. Kuroda, T. Osaka, *J. Mater. Chem.*, 15 (2005) 1987.

[16] H. Usui, Y. Yamamoto, K. Yoshiyama, T. Itoh, and H. Sakaguchi, *J. Power Sources*, 196 (2011) 3911.

[17] W. J. Weydanz, M. W. Mehrens, R. A. Huggins, *J. Power Sources*, 81–82 (1999) 237.

[18] P. Limthongkul, Y.-I. Jang, N. J. Dudney, Y.-M. Chiang, *Acta Materialia*, 51 (2003) 1103.

[19] H. Xia, S. Tang, L. Lu, *Mater. Res. Bull.*, 42 (2007) 1301.

[20] M. K. Datt, P. N. Kumta, *J. Power Sources*, 194 (2009) 1043.

[21] I. Ohno, *Mater. Sci. Eng. A*, 146 (1991) 33.

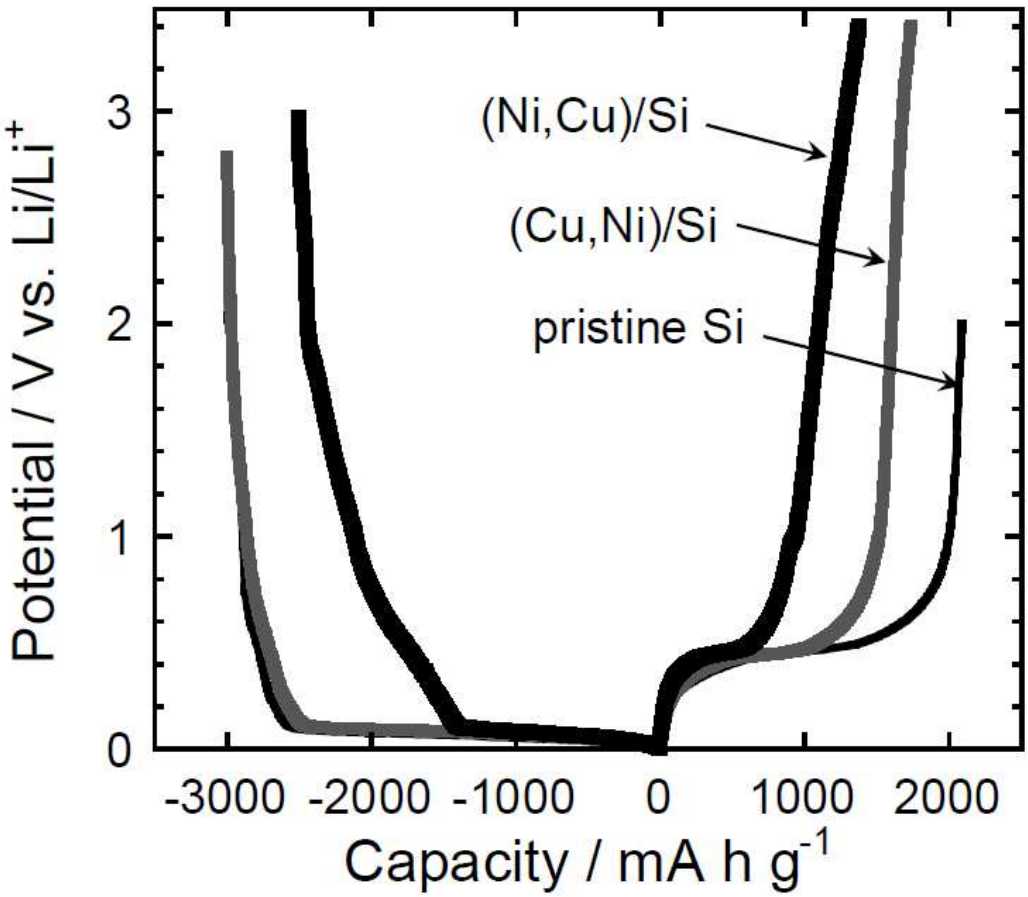

Fig. 1. Charge-discharge curves at the first cycles for thick-film electrodes consisting of pristine Si, (Cu, Ni)-coated Si, and (Ni, Cu)-coated Si particles. The (Cu, Ni) indicates coating number, primary ELD of Cu and successive ELD of Ni.

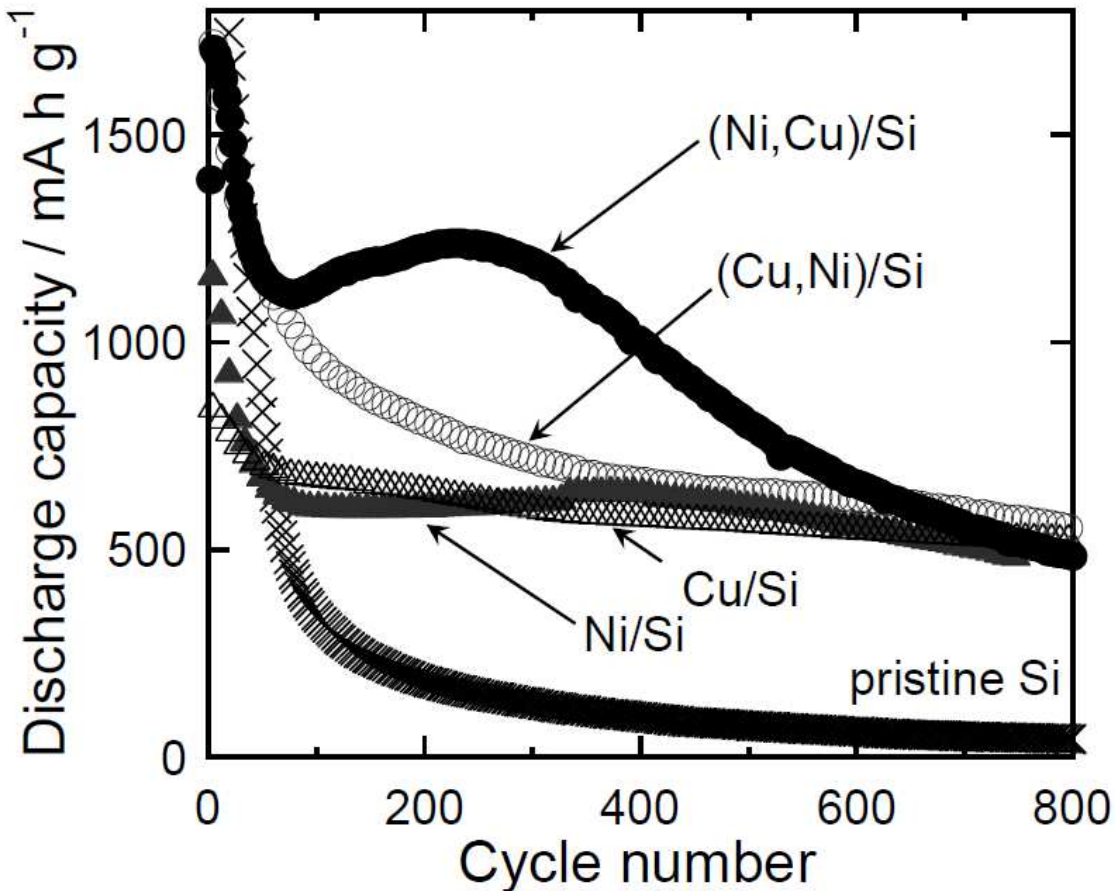

Fig. 2. Dependence of discharge capacity on charge-discharge cycling number in thick-film electrodes consisting of pristine Si, (Cu, Ni)-coated Si, and (Ni, Cu)-coated Si particles. For comparison, the capacities of Cu-coated Si and Ni-coated Si electrodes were shown in the figure. The first discharge capacity of the pristine Si electrode is 2000 mA h g^{-1}.

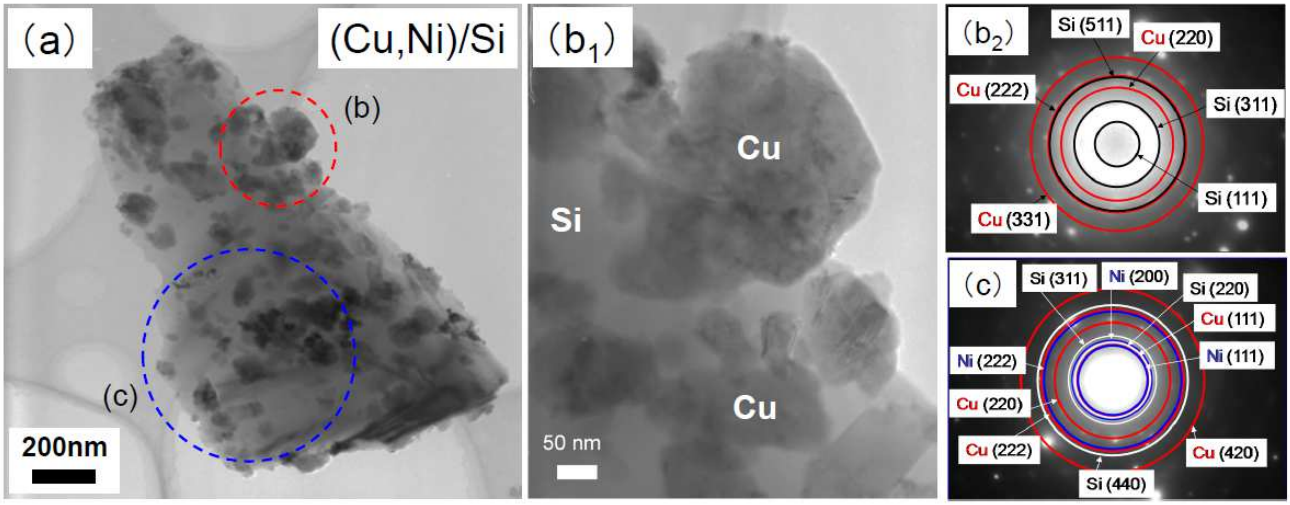

Fig. 3. (a) TEM image of (Cu, Ni)-coated Si particle prepared by ELD. (b_1) TEM image at high magnification and (b_2) corresponding selected area electron diffraction of (a). (c) Selected area electron diffraction for larger region of (a).

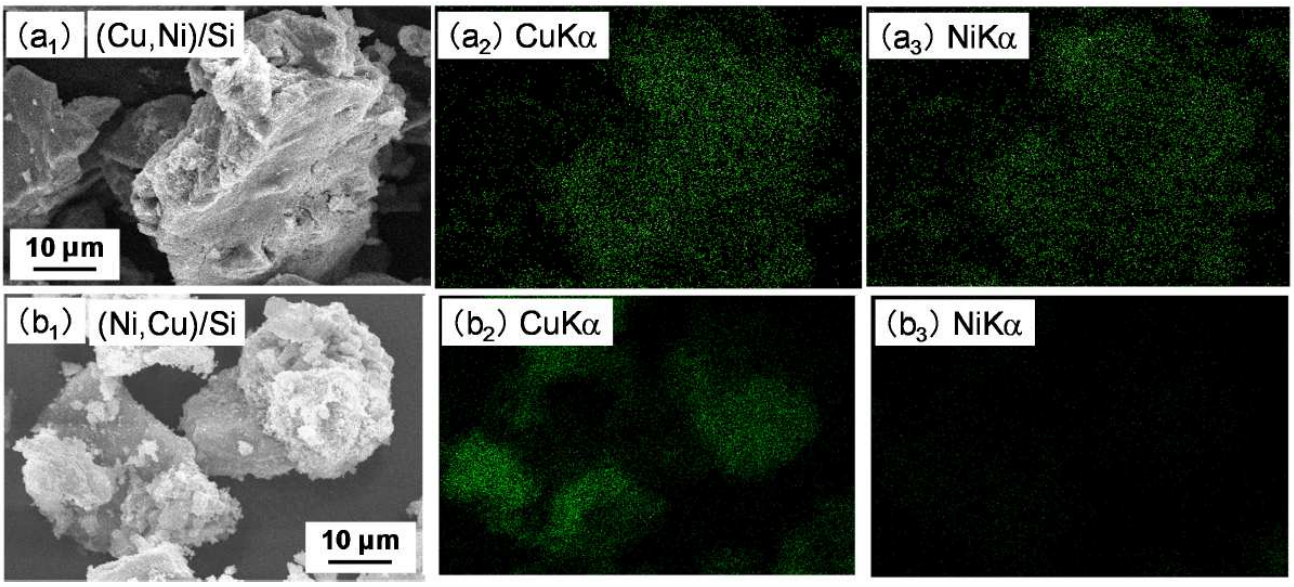

Fig. 4. (a_1) SEM image and corresponding element mapping of (a_2) Cu and (a_3) Ni for (Cu, Ni)-coated Si particles. (b_1) SEM image and corresponding element mapping of (b_2) Cu and (b_3) Ni for (Ni, Cu)-coated Si particles.

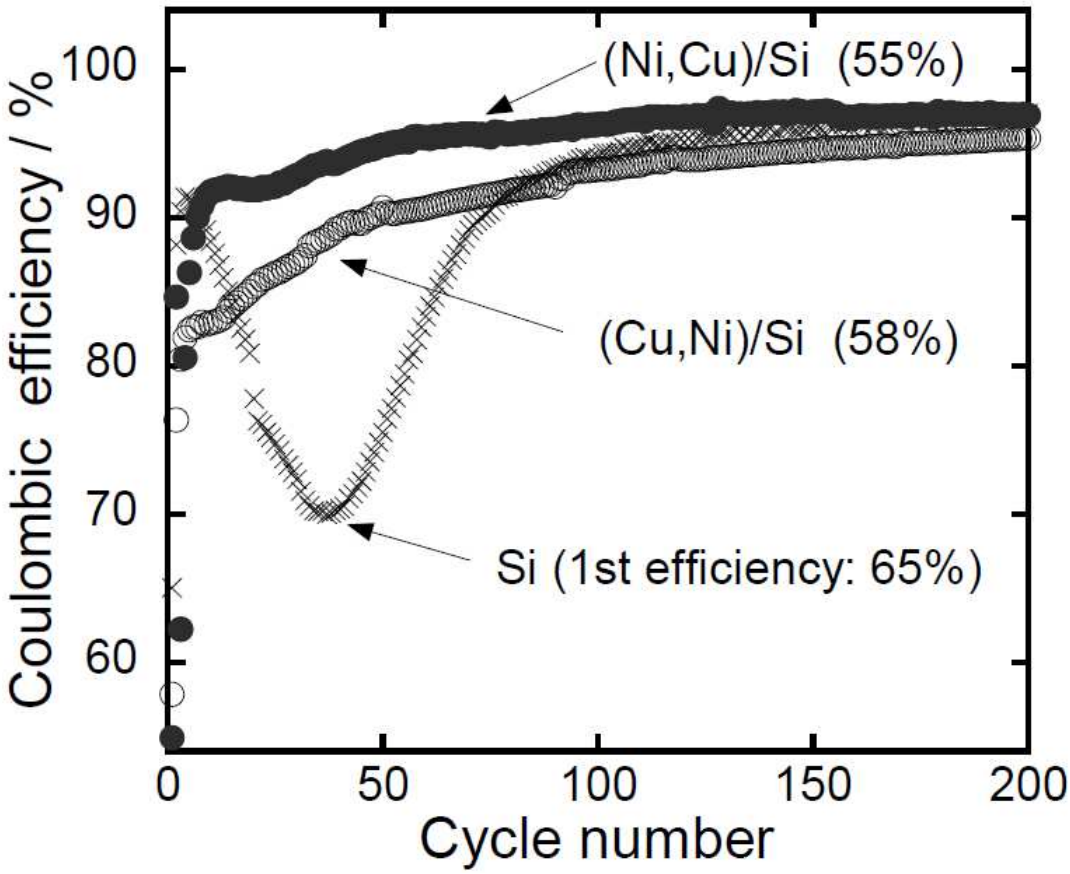

Fig. 5. Coulombic efficiencies of the thick-film electrodes consisting of (Cu, Ni)-coated Si and (Ni, Cu)-coated Si particles in the initial 200 cycles.

Figure captions

Fig. 1. Charge-discharge curves at the first cycles for thick-film electrodes consisting of pristine Si, (Cu, Ni)-coated Si, and (Ni, Cu)-coated Si particles. The (Cu, Ni) indicates coating number, primary ELD of Cu and successive ELD of Ni.

Fig. 2. Dependence of discharge capacity on charge-discharge cycling number in thick-film electrodes consisting of pristine Si, (Cu, Ni)-coated Si, and (Ni, Cu)-coated Si particles. For comparison, the capacities of Cu-coated Si and Ni-coated Si electrodes were shown in the figure. The first discharge capacity of the pristine Si electrode is 2000 mA h g^{-1}.

Fig. 3. (a) TEM image of (Cu, Ni)-coated Si particle prepared by ELD. (b_1) TEM image at high magnification and (b_2) corresponding selected area electron diffraction of (a). (c) Selected area electron diffraction for larger region of (a).

Fig. 4. (a_1) SEM image and corresponding element mapping of (a_2) Cu and (a_3) Ni for (Cu, Ni)-coated Si particles. (b_1) SEM image and corresponding element mapping of (b_2) Cu and (b_3) Ni for (Ni, Cu)-coated Si particles.

Fig. 5. Coulombic efficiencies of the thick-film electrodes consisting of (Cu, Ni)-coated Si and (Ni, Cu)-coated Si particles in the initial 200 cycles.